Earthquakes and Structures, *Vol. 13, No. 2 (2017) 119-130*
DOI: https://doi.org/10.12989/eas.2017.13.2.119

Seismic behavior of isolated bridges with additional damping under far-field and near fault ground motion

Daniele Losanno[*1], Houman A. Hadad[2a] and Giorgio Serino[1b]

[1]*Department of Structures for Engineering and Architecture, University Federico II, Via Claudio 21, 80125, Naples, Italy*
[2]*Department of Civil Architectural and Environmental Engineering, University of Miami, Florida, USA*

(Received December 13, 2016, Revised July 21, 2017, Accepted August 3, 2017)

Abstract. This paper presents a numerical investigation on the seismic behavior of isolated bridges with supplemental viscous damping. Usually very large displacements make seismic isolation an unfeasible solution due to boundary conditions, especially in case of existing bridges or high risk seismic regions.

First, a suggested optimal design procedure is introduced, then seismic performance of three real bridges with different isolation systems and damping levels is investigated. Each bridge is studied in four different configurations: simply supported (SSB), isolated with 10% damping (IB), isolated with 30% damping (LRB) and isolated with optimal supplemental damping ratio (IDB). Two of the case studies are investigated under spectrum compatible far-field ground motions, while the third one is subjected to near-fault strong motions. With respect to different design strategies proposed by other authors, results of the analysis demonstrated that an isolated bridge equipped with HDLRBs and a total equivalent damping ratio of 70% represents a very effective design solution. Thanks to confirmed effective performance in terms of base shear mitigation and displacement reduction under both far field and near fault ground motions, as well as for both simply supported and continuous bridges, the suggested control system provides robustness and reliability in terms of seismic performance also resulting cost effective.

Keywords: seismic response; isolated bridges; optimal design; near-fault; elastomeric bearings; supplemental damping

1. Introduction

Seismic isolation of new or existing bridges has been widely accepted and practiced in earthquake prone areas (Martelli and Forni 2010) and advanced now to a mature technology since recent earthquakes have given some insight into the actual performance of seismically protected bridges (Naeim 2000).

Isolation of bridge deck from piers is a convenient intervention for retrofit of existing bridges or design of new ones. In the present study, an isolation system with High Damping Laminated Rubber Bearings (HDLRBs) is introduced with 10% damping ratio (FIP Industriale 2016) and additional viscous dampers are provided to achieve higher levels of damping. In order to control the commonly large displacements of the isolated deck, supplemental damping system can be introduced properly designed to not increase transmitted force to the substructure.

To prove the effect of additional damping on isolated buildings, Kelly (1999) proposed a very effective dissertation on the role of damping on isolated structure. In this study, an elementary analysis based on a simple model of an isolated structure was used to demonstrate this effect. The result was that even if supplemental damping significantly reduces isolators' displacements, inter-story drifts and accelerations may increase. As demonstrated in the present paper, isolated bridges are expected to be less sensitive to this problem because of predominance of the first vibration mode.

Isolation technology has been widely adopted and proved advantageous in case of retrofit to achieve continuous functionality during a seismic event, especially for mission critical structures (Chen and Duan 2014). However, in case of existing bridges, seismic design displacements combined with thermal expansions to be accommodated through expansion joints can be many times higher than the practical clearance between the decks, thus resulting pounding and unseating as major concerns (Pantelides and Ma 1998). As alternative solutions, change of deck configuration or increase of available clearances would imply a downtime and higher cost.

Another important design issue of isolated bridges is their performance under near-fault ground motions. This topic became a matter of concern especially after Northridge Earthquake in 1994 where isolated structures constructed in the vicinity of San Andreas Fault were subjected to long-period displacement pulses with high velocity contents, duration of which matched the isolated period of the structure and caused excessive displacement responses (Liao *et al*. 2004, Jangid and Kelly 2001, Shen *et al*. 2004, Jònsson *et al*. 2010). Different studies show that devastating effects of near-fault earthquakes on isolated bridges are first due to characteristics of displacement pulse

∗Corresponding author, Ph.D.
E-mail: daniele.losanno@unina.it
[a]Ph.D. Candidate
E-mail: houman@umiami.edu
[b]Professor
E-mail: serino@unina.it

ISSN: 2092-7614 (Print), 2092-7622 (Online)

which is commonly long-period and large at peak and, second, because of the high velocity content of the pulses that are in the order of magnitude of 1 m/s. Hence, near-fault ground motions are most likely to affect both structures with long natural period range like isolated structures and structures sensitive to velocity content such as viscously damped structures.

Not surprisingly, the isolation technology under near-fault motion was firstly criticized by the academia (Hall *et al*. 1995), but then it became an appealing research subject and many studies proposed different ways to overcome the poor performance using Shape Memory Alloys (Ozbulut and Hurlebaus 2010), using Magneto Rheological Dampers (Sahasrabudhe and Nagarajaiah 2005) or optimizing Lead Rubber Bearings (Jangid 2007).

Makris and Chang (2000) examined the effectiveness of various dissipative mechanisms to protect structures from pulse-type and near-source ground motion. The study considered one or two degree of freedom systems and concluded that a combination of relatively low friction and viscous force is practical since base displacements are substantially reduced without significantly increasing base shear and superstructure acceleration. They found that at low isolation period range (T_i<2 s) additional viscous damping reduces displacements and base shear in the most effective way. At high isolation period ranges, friction dissipation becomes effective in reducing displacement response, however, the resulting base shear is the larger. For isolation period T_i>2 s, viscous dissipation results in large displacements that are substantially reduced when some friction dissipation is introduced. Friction dissipation eliminates amplification due to resonance for isolation periods larger than 2 s.

Losanno *et al*. (2014) implemented a frequency domain approach for damping optimization in both elastomeric viscoelastic and sliding isolators on regular bridges. In case of elastomeric isolators, the authors introduced a dimensionless optimum viscous damping parameter (ν_i) as a function of piers to isolation system relative stiffness (κ). They demonstrated that increasing the damping level of the isolation system is not always favorable and there exists an upper limit for the damping level, after which no benefit is gained from increasing the damping ratio. Thus, it is possible to define an optimum damping ratio that minimizes the deck displacement.

Based on the latter study, this paper presents a numerical investigation on real bridges assumed to be designed with elastomeric isolators and different levels of damping. The theoretical basis of the proposed design procedure is described in the second chapter where main assumptions of the method are explained. Then, the design procedure was applied to three benchmark bridges (namely BM#1, BM#2, BM#3), assuming far-field and near-fault ground motions. In each case study, four configurations of simply supported non-isolated bridge with 5% damping (SSB configuration), isolated bridge with 10% damping produced by HDLRB isolation system (IB configuration), isolated bridge with 30% damping produced by Lear Rubber Bearings (LRB configuration), and isolated bridge with optimized viscous damping ratio (IDB configuration) are examined.

Time history analysis are performed to provide an estimation of the structural response on simplified 2 degree of freedom (DOF) models. Input frequency content on the overall response was also taken into consideration. As demonstrated in the following, 2 DOF models did not alter the scope of the work.

Finally, considerations on cost evaluation of the proposed isolation system with additional damping are provided in order to assess effectiveness with respect to classical solutions.

2. Theoretical framework of optimally-designed ısolation system

Theoretical basis of optimally damped seismic isolation systems for regular bridges is taken from the study of Losanno *et al*. (2014) and herein briefly presented. Assuming an undamped behavior of the piers, the authors demonstrated that a certain level of damping could be effective in reducing the super-structure displacements while not increasing or furtherly reducing base shear. The dynamic behavior of a multi-span simply supported linear elastic isolated bridge with variable additional damping level was investigated. As illustrated in Fig. 1, the deck was reduced to a lumped mass *m* and the piers represented by linear springs of stiffnesses $k_{c,j}$ and masses $m_{c,j}$. Isolators were accordingly modelled with linear springs of stiffnesses $k_{i,j}$ in parallel with dashpots of damping coefficients c_j. Under assumptions of negligible participating mass of piers and isolators with equal stiffness and damping properties (regular bridge), the rheological model presented in Fig. 1(a) was reduced to the one of Fig. 1(b) that simplifies the real bridge by concentrating the total mass of the piers m_c and the deck *m*, thus providing a 2 DOF system. Linear springs with stiffnesses $k_c = n \times k_{c,\mathrm{j}}$ and $k_i = n \times k_{i,\mathrm{j}}$ (j-th pier stiffness $k_{c,\mathrm{j}}$, j-th isolator stiffness $k_{i,\mathrm{j}}$) represent the total lateral stiffness of the piers (i.e., bridge lateral stiffness in non-isolated configuration) and the isolation system, respectively. The total damping of the isolation system and supplemental dampers is lumped in a dashpot with damping coefficient $c = n \times c_j$. Under further assumption that m_c is negligible with respect to *m*, the model of Fig. 1(b) can be reduced to a single-dynamic-degree-of-freedom of mass *m* and two kinematic-degree-of-freedoms x_c (piers displacement) and x (deck displacement).

Dynamic response was obtained under harmonic excitation with frequency $\bar{\omega}$, in terms of normalized deck displacement as a function of normalized parameters as follows:

- exciting frequency $\beta = \bar{\omega} / \omega_i$
- relative pier to isolation stiffness $\kappa = \dfrac{k_c}{k_i}$
- viscous damping ratio $\nu_i = \dfrac{c}{2m\omega_i}$.
- isolation frequency $\omega_i = \sqrt{k_i / m}$

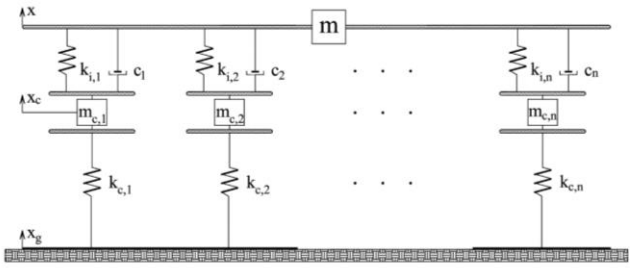

(a)

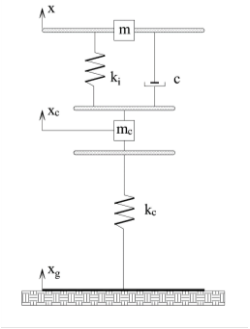

(b)

Fig. 1 Rheological model of isolated bridges: (a) Multi-support and (b) simplified

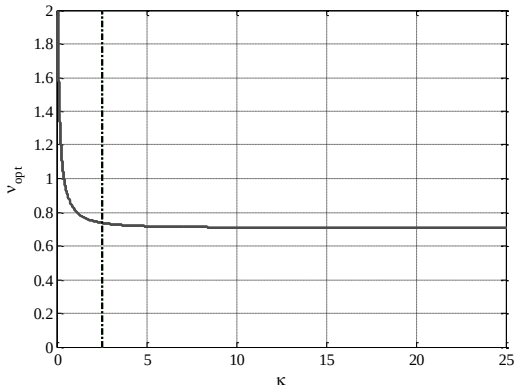

Fig. 2 Optimum damping ratio over stiffness ratio κ

Given a certain target isolation period $T_i = \frac{2\pi}{\omega_i}$, Losanno *et al*. (2014) found a closed form expression for the optimum damping ratio $\nu_{i,opt}$ that minimizes the maximum deck displacement over the overall range of frequency, as a function of the only relative stiffness ratio through the relation (1) plotted in Fig. 2

$$\nu_{i,opt} = \sqrt{\frac{(1+\kappa)^2}{2\kappa(2+\kappa)}} \tag{1}$$

A very interesting outcome was that the optimum damping ratio converged to a point approximately equal to 0.70 for stiffness ratios κ>2.5 (vertical grey line in Fig. 2), i.e., when isolated $T_i = 2\pi\sqrt{m/k_i}$ to simply supported $T_c = 2\pi\sqrt{m/k_c}$ structural period ratio T_i/T_c is larger than $\sqrt{2.5} \approx 1.6$. This value would correspond to a very common condition for real bridges.

The suggested procedure was numerically validated on a regular bridge with 2.5 s isolation period, demonstrating that $\nu_{i,opt}$ also corresponded with very good accuracy to minimum base shear. However, applicability of the procedure to real bridges, near fault ground motion response and economical sustainability were not taken into account.

As an advancement of the referred work, the equivalent stiffness of a non-regular bridge with *n* different supports could be written as

$$k_{eq} = \sum_{j=1}^{n} \frac{k_{c,\mathrm{j}} \cdot k_{i,\mathrm{j}}}{k_{c,\mathrm{j}} + k_{i,\mathrm{j}}} \tag{2}$$

which in case of regular bridge yields

$$k_{eq}^{reg} = n \cdot \frac{k_{c,j} \cdot k_{i,j}}{k_{c,j} + k_{i,j}} = \frac{k_c \cdot k_i}{k_c + k_i} \tag{3}$$

where $k_c = \sum_{j=1}^{n} k_{c,\mathrm{j}}$ and $k_i = \sum_{j=1}^{n} k_{i,\mathrm{j}}$.

In the general case of non-regular bridges, the stiffness k_{eq}^{reg} from Eq. (3) only approximates k_{eq} from Eq. (2), with a relative error $\epsilon = (k_{eq}^{reg} - k_{eq})/k_{eq}$. In all practical cases where seismic isolation is effective, the parameter κ is high and the error ϵ is expected to be low so that the simplified model of Fig. 1(b) would be suitable for prediction of global seismic behavior. Therefore, the stiffness ratio κ and the corresponding damping level $\nu_{i,opt}(\kappa)$ were calculated for a real bridge assuming $k_c = \sum_{j=1}^{n} k_{c,\mathrm{j}}$ and $k_i = \sum_{j=1}^{n} k_{i,\mathrm{j}}$.

In addition, since the solution $\nu_{i,opt}(\kappa)$ approaches an asymptotic value for any practical value of κ, as demonstrated in the following, the value of 70% could be taken as reference even for non- regular bridges.

In the following chapter, numerical analysis are implemented on simplified 2 DOF models of benchmark bridges provided with an isolation system with different levels of damping ratios, including the optimal one $\nu_{i,opt}(\kappa)$. It will be shown that at least in a preliminary design step, the real bridge can be simplified by the equivalent model of Fig. 1(b) and that the suggested level of additional damping substantially improves seismic performance of the isolated deck.

3. Design of ısolated bridges with supplemental damping system

In the following, effectiveness of the proposed design strategy is studied for three bridges analyzed in four configurations namely simply supported (SSB), isolated by HDLRBs with conventional 10% damping (IB), isolated by LRBs with equivalent 30% damping (LRB) and isolated by HDLRBs with optimal damping ratio (IDB).

Dynamic properties of the bridge are determined in both fixed and isolated configuration, then its response in terms of displacement, elastic force, damping force and base shear is obtained for each mock-up under a set of scaled or real ground motions.

Isolators were designed to achieve a fixed target period (2 to 2.3 s) and were checked in terms of stability conditions, i.e., rollout displacement and vertical buckling load.

At the preliminary design step, the displacement demand was obtained as corresponding to the target natural period for the expected level of damping.

HDLRBs were assumed to provide up to 10% damping ratio to the structure (Fip Industriale 2016), assuming that in IDB system additional dampers are supplied to achieve higher levels of damping.

For preliminary design of HDLRBs, spectral displacements were estimated by correction factors $\eta = \sqrt{10/(5+\nu)}$ (EC8 2004, NTC 2008) or $B_L = (\nu/_{0,05})^{0,3} \leq 1,7$ (AASHTO 2010) for the expected level of damping. These factors would be limited for threshold values of damping around 30% ($\eta \leq 0,55$, $B_L \leq 1,7$), with the aim to discourage practitioners from using simplified spectral analysis with higher damping levels. For the purpose of preliminary design, a rough estimate of spectral displacements for the expected level of damping can be assumed by aforementioned reduction factors, practically neglecting upper boundary fixed by the Code. This assumption on displacement demand was always checked by means of time history direct integrations analysis.

An advantage of increasing the damping and, accordingly, reducing the response displacement, was reduction of total rubber thickness of bearings. The latter was directly related to the design maximum displacement through the relation $t_r = \frac{d_{\max}}{\gamma_{\max}}$ (Kelly 1997) where $d_{\max}$ is the spectral displacement considering 50% increase to take reliability of the isolation technology into account (EC8 2004), and γ_{max} is the maximum shear strain. From this perspective, it can be deemed that supplemental damping leads to more stable and economical devices and this effect is explicitly taken into account for the design and the cost evaluation of different IB and IDB solutions.

LRBs were assumed to provide equivalent damping levels up to 30% through yielding of the lead core. Hysteresis behaviour of LRB is usually modelled as bilinear, where initial stiffness is provided by lead core while after yielding residual stiffness is mainly due to rubber. For the sake of comparison, in the present work a simplified linear equivalent model with secant stiffness and damping ratio around 30% at design displacement is assumed for time-history analysis.

In the design process, stability checks limited the excessive horizontal displacement and buckling, as discussed in the work of Kelly (1997). Finally, the maximum horizontal shear strain was limited to 5.5 according to AASHTO (2010), taking into account effects of rotation in the elastomer, seismic horizontal loads and compressive stress.

In the following, a maximum strain level $\gamma_{\max}$ between 100 and 200% and corresponding equivalent modulus $G(\gamma_{\max}) = 0.4mPa$ were assumed depending on design objective.

The optimum damping ratio $\nu_{i,opt}(\kappa)$ was estimated assuming $k_c = \sum k_{c,j}$ (i.e., total lateral stiffness of the non-isolated bridge) and $k_i = \sum k_{i,j}$ (i.e., total lateral stiffness of the isolation system).

Two DOF models of three benchmark bridges were investigated by time-history analysis with direct time integration Newmark-Beta method using OpenSees (2016) program.

BM#1 is an existing simply supported bridge in Italy. BM#2 is a multispan continuous bridge taken from reference (Buckle and Monzon 2011) and proposed by other authors with an LRB system. BM#3 is taken from a further reference (Wang *et al*. 1998) of a three-span continuous bridge seismically isolated under near fault ground motion.

3.1 Case study #1

The first case study is an example of multi-span simply supported highway bridge located in south of Italy (Vallata (AV), about 100 km from Naples). The reinforced concrete deck is 2 m height with prestressed beams and upper concrete slab. As shown in Fig. 3, the bridge has two lanes with five equal-in-length spans of 33.4 m, separated by thermal joints approximately 20 cm width. A single span of the east line is adopted for seismic analysis in the longitudinal direction. The structure was designed to act as pinned on one pier and roller-supported on the other one to consider the thermal expansion. Properties of the bridge for a single span are summarized in Table 1.

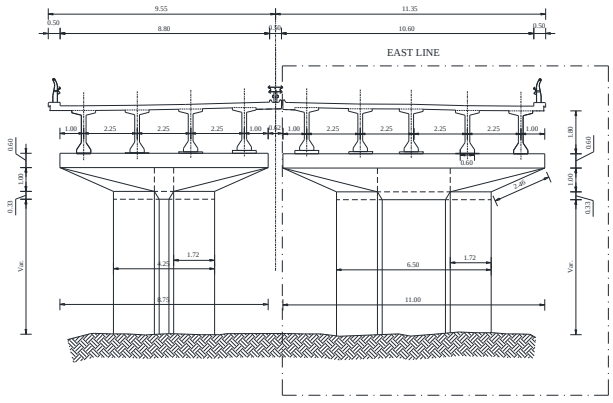

Fig. 3 Transverse cross section and details of BM#1

Table 1 Properties of SSB for BM#1

Horizontal Stiffness k_c	547582	kN/m
Weight of the Super Structure	6741	kN
Total Seismic Weight	7413	kN
Piers' mass to total mass percentage	9	%
Horizontal Natural Period	0.16	s

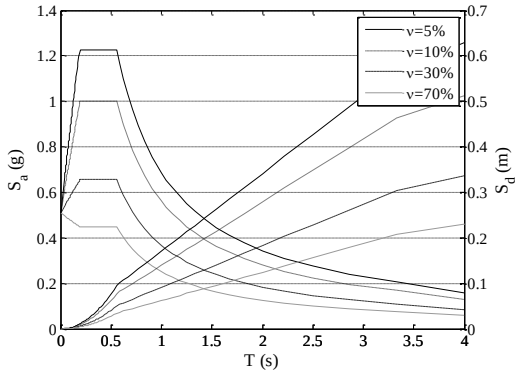

(a) Elastic Spectrum according to NTC 08

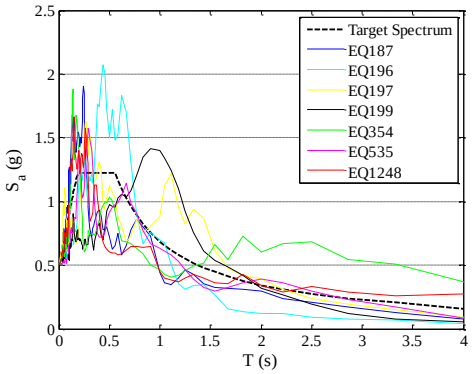

(b) Scaled input ground motion

Fig. 4 Design Spectrum for BM#1

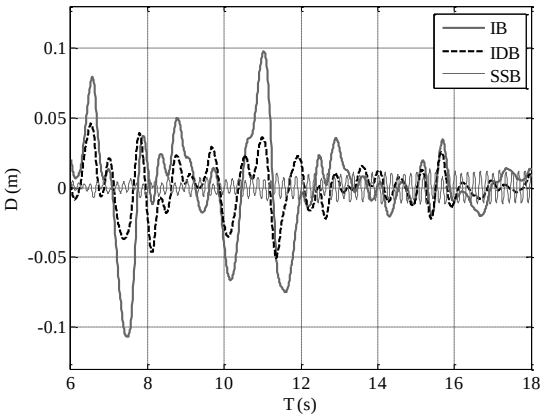

(a) displacement

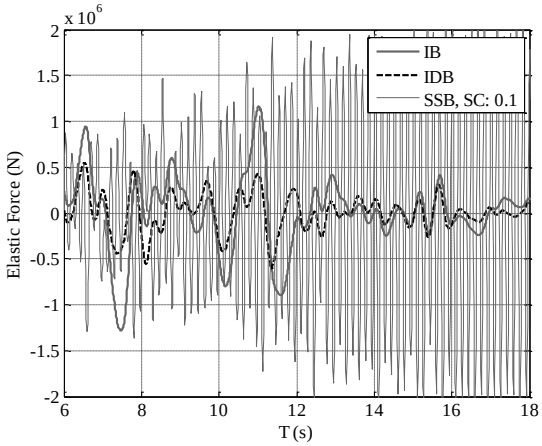

(b) elastic force

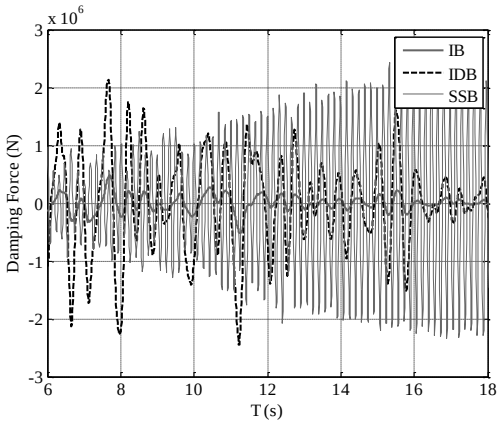

(c) damping force

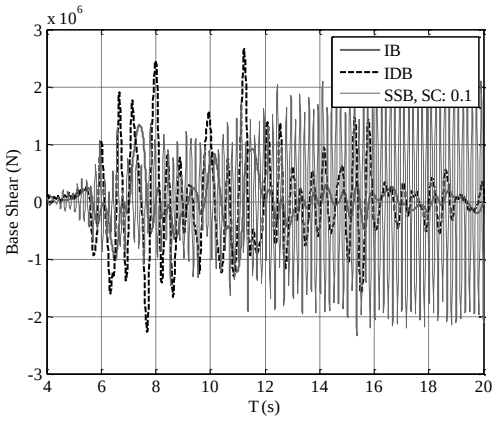

(d) base shear

Fig. 5 Response of BM#1 under Montenegro-196 Earthquake

The design spectrum for collapse prevention limit state (SLC) is obtained according to latest Italian seismic provisions (NTC 08) and shown in Fig. 4(a). The bridge is located on topographic area T1 and soil type B with nominal life equal to 100 years and importance class IV, corresponding to a return period of 2475 years.

A target isolation period of 2 s was fixed, to which an equivalent stiffness of 7421 kN/m corresponded as provided by 10 equal bearings. Maximum shear strain of rubber compound was assumed 200%. Based on a target displacement of 0.41 m, the design of IB provided a diameter of the single device equal to 0.70 m.

Such a simple case exactly matches the assumptions for regular bridge, so that $k_{eq} = k_{eq}^{reg}$. The optimum damping of this bridge was found to be 70% by Eq. (1), based on the stiffness ratio $\kappa = {}^{547582}/_{7421} \cong 74$.

Despite the IB case, IDB system is assumed to be obtained adopting HDLRBs and supplemental viscous dampers for a total damping ratio of 70%. Thanks to a

Table 2 Input ground motion for BM#1

Waveform ID	Earthquake Name	Mw	Scale Factor	Fault Mechanism	Epicentral Distance [km]	PGA_X [m/s^2]	PGV_X [m/s]
535	Erzincan	6.6	0.55	strike slip	13	3.8142	1.0177
1248	Izmit	7.6	1.12	strike slip	55	2.0473	0.0957
187	Tabas	7.3	1.73	oblique	57	9.0835	0.8443
196	Montenegro	6.9	1.36	thrust	25	4.453	0.388
197	Montenegro	6.9	3.17	thrust	24	2.8797	0.3861
199	Montenegro	6.9	0.99	thrust	16	3.6801	0.421
354	Panisler	6.6	4.05	strike slip	33	1.2389	0.3688
mean:	-	6.97	1.85	-	31.85	3.88	0.50

lower value of design displacement (0.18 m), a smaller diameter of 0.47 m was obtained for the single bearing. Spectral displacements with aforementioned correction factors suggest a reduction of approximately 50% passing from 10% to 70% damping ratio.

In order to investigate dynamic behavior of the structure in different configurations, time-history analysis was performed with a set of seven scaled spectrum compatible scaled ground motions selected from Rexel v.3.5 data base (Iervolino *et al*. 2010). Ground motions were selected to match soil class of the site and its target spectrum in the period range between 1 and 3 seconds in accordance with the target period of the isolated bridge. Average of the seven input spectrum did not exceed 10% upper and lower bound eccentricity tolerances from the given target spectrum. Table 2 provides information about the input ground motions which are graphically illustrated in Fig. 4(b).

With the aim to understand the behavior of systems with different levels of viscous damping, a sample response of the bridge under #196 motion in the time interval 6 to 18 seconds is shown in Fig. 5 for IB, IDB and SSB configurations.

As expected, increasing natural period of the system from 0.16 to 2 s considerably increases displacement response (Fig. 6(a)). This effect, especially at peaks, is significantly controlled in case of IDB. Reduction of displacement response along with increasing flexibility of the isolated deck, strongly decreased the elastic force in the system, evident in Fig. 6(b), where elastic force for SSB is scaled to one-tenth of the original for convenience. Viscous force (Fig. 6(c)) was maximum in IDB due to high value of damping coefficient. However, the total base shear in Fig. 6(d) was significantly reduced in isolated configurations, either with or without supplemental damping.

Comparing Fast Fourier Transforms (FFTs) of the deck acceleration in Fig. 6 confirms the variability of the response, particularly in case of IDB where frequency content is very similar to input ground motion due to high viscous damping ratio. While in the case of SSB and IB the peak of FFT occurs at system natural frequencies i.e., 6 Hz

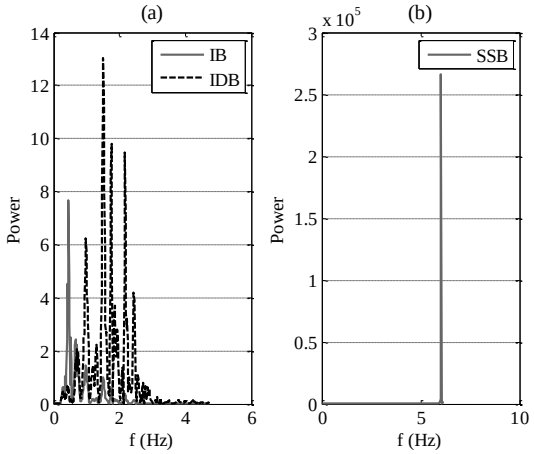

Fig. 6 Accelerations FFT for eq. #196: (a) IB and IDB, (b) SSB

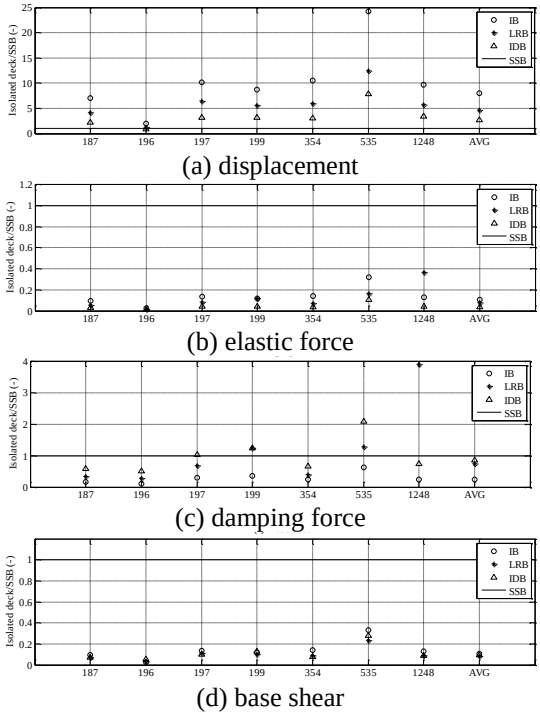

(a) displacement

(b) elastic force

(c) damping force

(d) base shear

Fig. 7 Normalized maximum values of BM#1 response

and 0.5 Hz, respectively, FFT function for IDB did not provide a single dominant frequency.

Bridge response in SSB, IB, LRB and IDB configurations was determined under each input ground motion. By analyzing seven independent ground motions, design response values are defined as the average of maxima.

Output response for each ground motion is illustrated in Fig. 7 both in terms of normalized maxima and corresponding average. Under some earthquakes, IB displacement increased more than 10 times SSB displacement: introduction of IDB notably limited this magnification as given in Fig. 7(a).

Thanks to isolated deck, pier displacement and elastic force are strongly reduced, as evident from Fig. 7(b), while

Table 3 Cost evaluation for BM#1 and comparison with IB

	Islators cost	Dampers cost	Total	Difference
IB	€83,448	€	€83,448	0%
LRB	€100,137	€	€100,137	20%
IDB	€26,569	€36,643	€63,212	-24%

damping force in IDB is undoubtedly higher than IB (Fig. 7(c)).

A comparison between isolated deck solutions highlights that peak value of base shear depends on ground motion and its frequency content. Nevertheless, the difference between IB, IDB and LRB in terms of absolute base shear is trivial if compared to remarkable reduction with respect to SSB. Avarage base shear and accelerations for IB, LRB and IDB are almost equally reduced of 90% with respect to SSB (Fig. 7(d)).

As a summary of results, design of IDB allows to reduce displacement demand of 65% with respect to IB (i.e., from 0.20 m to 0.07 m) and 42% with respect to LRB (i.e., from 0.12 m to 0.07 m).

In order to evaluate the economical convenience of the different solutions, the italian price list issued by public ministry for highway construction and management (ANAS 2016) was employed to estimate the cost of devices in different isolation configurations, neglecting influence of local connections. Unitary cost is provided in terms of isolator size and maximum damper force, with an additional cost of 20% for lead core bearings with respect to elastomeric ones. As a first estimate, LRBs were assumed the same dimensions of corresponding IB.

With respect to IB (i.e., HDLRB isolators with 10% damping), IDB (HDLRB isolators with 10% damping + dampers providing additional 60% damping) was expected to be more expansive due to use of supplemental dampers that may considerably increase the cost of the protection system. In spite to this, in IDB the cost of HDLRBs tends to reduce thanks to lower size for limited displacement demand.

The economic assessments are summarized in Table 3. The proposed solution proved to be cost-effective with 24% saving in IDB case. Needless to mention that the benefits gained from more than 50% reduced design displacements were even much more valuable.

3.2 Case study #2

Benchmark bridge #2 is a continuous 3-span steel plate-girder structure with single column piers and seat-type abutments (Buckle and Monzon 2011). Total length of the bridge is 110.5 m having two lateral spans of 32 m and a middle span of 46.5 m. The bridge is located and originally designed in the United States. Transverse cross section and plane view are illustrated in Figs. 8 and 9, respectively. The height of the superstructure is approximately 7.31 m above the ground. Dynamics properties of the bridge in fixed deck configuration (SSB) are provided in Table 4.

In the original reference study, an isolation system is proposed using LRB in compliance with the AASHTO -

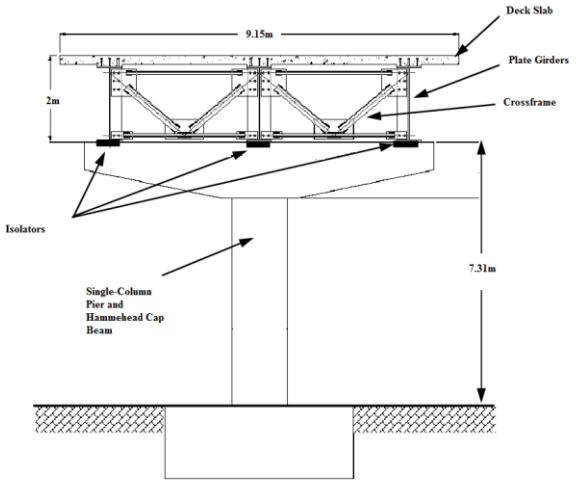

Fig. 8 Cross-section of BM#2

Table 4 Details of SSB configuration for BM#2

Horizontal Stiffness	101177.7	kN/m
Weight of the Super Structure	7345	kN
Total Seismic Weight	8485	kN
Piers' mass to total mass percentage	13.5	%
Horizontal Natural Period	0.58	s

Guide Specifications for Seismic Isolation Design (AASHTO 2010) consisting of 12 bearings providing an equivalent damping of 31% at 2.3 s target period. This configuration, namely LRB, is also taken into account for the sake of comparison.

IB system was designed for the same target period and a maximum shear strain of 200%: for a spectral displacement of 0.42m, a bearing diameter of 0.59 m and a total isolation stiffness of 6377 kN/m were obtained.

By Eq. (1) the optimal damping corresponding to a stiffness ratio $\kappa = \frac{101177.7}{6377} = 15.8$ is 70%, with an error $\varepsilon = 4{,}5\%$.

Thanks to a 70 % damping ratio, the isolation system in IDB configuration was designed for a displacement level of 0.23 m that provided a single isolator diameter of 0.44 m.

Seismic hazard at the site is defined by reference (Buckle and Monzon 2011). Response spectra for different levels of damping are plotted in Fig. 10(a).

For dynamic analysis, a set of seven scaled spectrum-compatible ground motion were selected from PEER Ground Motion Data Base (Chiou *et al*. 2008). Ground motions were matched to the soil class at the site and are selected from the magnitude interval of [5, 8] with a scale factor in the range 0.5 to 2.

Table 5 summarizes ground motion selection from PEER database that is plotted in Fig. 10(b).

Under each input motion, maximum values of response at the bridge deck as well as corresponding elastic force, damping force and total base shear were calculated. Results are presented in Fig. 11, where maxima were normalized

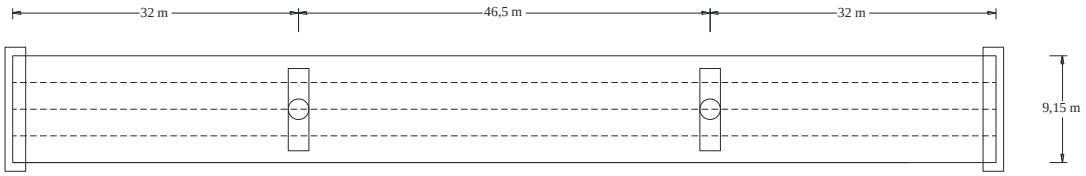

Fig. 9 Plane view of BM#2

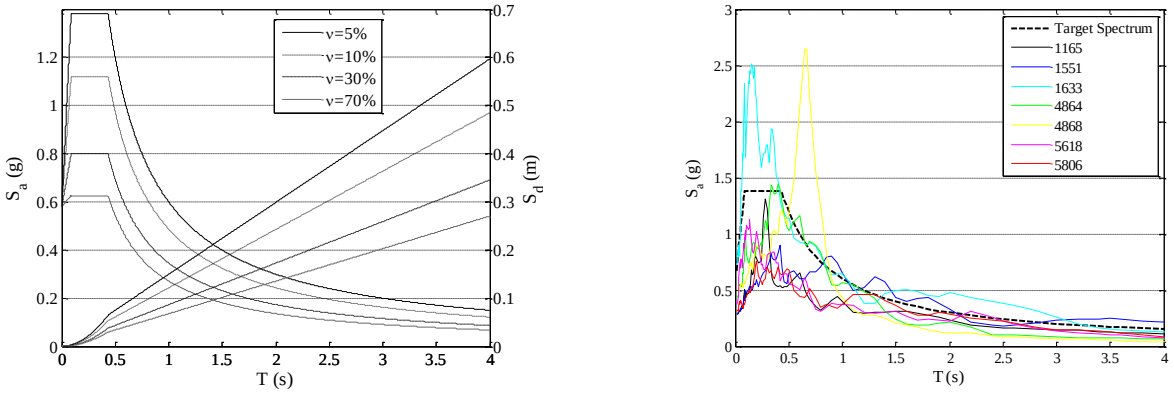

(a) Elastic Spectrum according to AASHTO (b) Scaled input ground motion

Fig. 10 Design Spectrum for BM#2

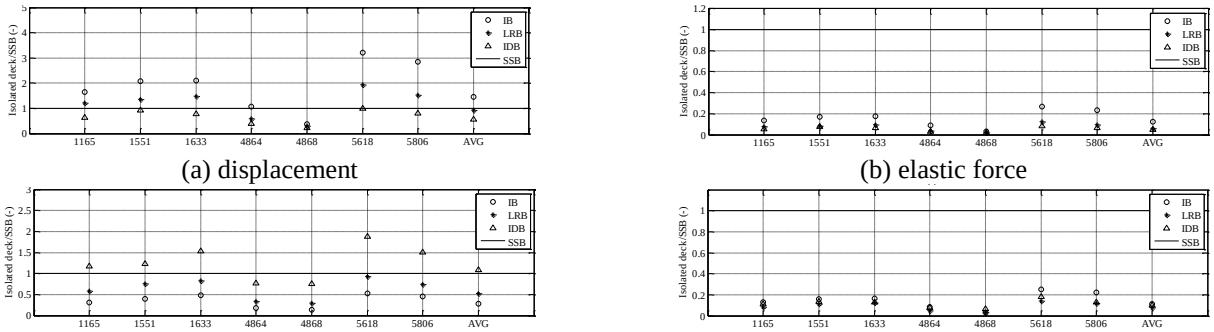

(a) displacement (b) elastic force

(c) damping force (d) base shear

Fig. 11 Normalized maximum values of BM#2 response

Table 5 Input Ground Motion for BM#2

Waveform ID	Earthquake Name	Country	Mw	Scale Factor	Fault Mechanism	Distance to Rupture Plane [km]	PGA_X [m/s^2]
1165	Kocaeli	Turkey	7.51	1.59	strike slip	7.21	4.42
1551	Chi-Chi	Taiwan	7.62	1.23	Reverse Oblique	9.78	3.59
1633	Manjil	Iran	7.37	0.80	strike slip	12.55	5.74
4864	Chuetsu-oki	Japan	6.8	1.35	Reverse	16.1	5.74
4868	Chuetsu-oki	Japan	6.8	1.56	Reverse	28.12	7.46
5618	Iwate	Japan	6.9	1.56	Reverse	16.27	5.7
5806	Iwate	Japan	6.9	1.59	Reverse	25.56	4.87
mean:	-		7.1285	1.38	-	16.15	5.36

with respect to corresponding values of SSB.

Displacement response values (Fig. 11(a)) of the bridge were generally increased when isolation was used. The odd structural behavior under motion #4868 can be explained considering that input acceleration peaked at almost 2.5 g for the period of 0.6 s (Fig. 10(b)) producing approximately 0.3 m displacement in SSB. Note that ground motions were selected not to violate allowable eccentricity tolerance from the target spectrum in the period interval of isolated bridge, which is from 1 to 3 s, therefore a larger scatter at SSB period resulted.

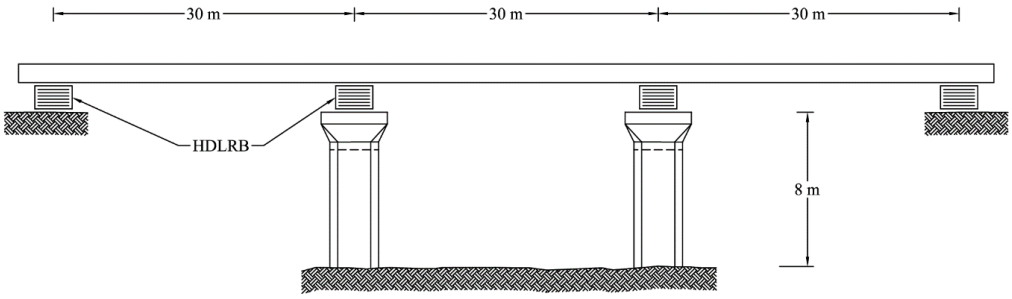

Fig. 12 Schematic view of BM#3

Table 6 Cost evaluation for BM#2 and comparison with IB

	Islators cost	Dampers cost	Total	Difference
IB	€74,768	€	€74,768	0%
LRB	€89,722	€	€89,722	20%
IDB	€34,510	€25,700	€60,210	-19%

Table 7 Details of SSB configuration for BM#3

Horizontal Stiffness	155025	kN/m
Weight of the Super Structure	7623.5	kN
Total Seismic Weight	8008.7	kN
Piers' mass to total mass percentage	4.8	%
Horizontal Natural Period	0.46	s

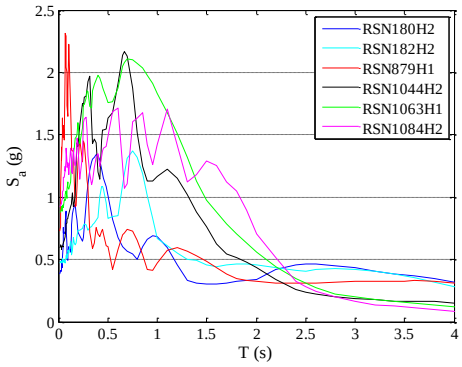

Fig. 13 Input ground motion for BM#3

By neglecting ground motion #4868, it should be also marked that the increase in normalized displacement response in IB configuration was moderated from an average of almost 8 in BM#1 to an average of approximately 2.5 in BM#2. This is mainly due to the higher natural period of SSB in BM#2 (0.58 s vs 0.16 s) that was translated in a lower value of κ.

If eq. #4868 was not taken into account, LRB displacement would be approximately 50% and 90% higher than SSB and IDB, respectively.

Regardless of the configuration, isolated deck produced a base shear decrease of approximately 90%.

IDB damping force always peaked at higher values than IB as shown in Fig. 11(c).

An extended model of the bridge was also implemented in SAP2000 to evaluate the approximation introduced with the simplified 2 DOF model. The error in the average of maximum displacements was only 1.7 % which confidently validated the simplified model.

As in the previous case, cost of IDB configuration was the least if compared with IB and LRB (Table 6). This means that in IDB, despite the additional cost of dampers, isolators would be cheaper thanks to the reduced bearing size.

3.3 Case study #3

A third benchmark bridge was analyzed in order to investigate the effectiveness of additional viscous damping under near-fault ground motions.

This bridge was first mentioned in the work of Wang *et al.* (1998), to study the response of Friction Pendulum Bearings (FPS) and then referred in the study of Jangid (2007) where the target was to find the optimum parameters of an LRB system. In particular the aim of Jangid (2007) was to find the optimal ratio of stiffness to hysteretic damping for a near-fault motion. The case study is a three equal-span continuous concrete bridge, totally 90 m long with two central piers of 8 m height having cross section area of 4.09 m^2 and moment of inertia of 0.64 m^4, for a total of 8 bearings. Both abutments are assumed to be fixed. Details are given in Table 7 while Fig. 12 shows a schematic drawing of the bridge.

Since near-fault records were considered in this case, no spectral matching was conducted for ground motion selection. A certain value of response displacement was assumed for preliminary design of the elastomeric bearings which was 0.4 m for IB and half of that for IDB. These values were checked with time history results. In order to meet stability criteria, maximum shear strain in the isolator was limited to 100% with a target isolation period of 2.5 s corresponding to an equivalent stiffness of 5134 kN/m.

Stiffness ratio was computed equal to $\kappa = \frac{155025}{5134} = 30$

and the error in calculating k_{eq}^{reg} instead of k_{eq} arised to 2,4%. Also in this case, corresponding optimal damping ratio by Eq. (1) was $\nu_{i,opt} = 0.70$.

In order to accommodate such a large design displacement, diameter of HDLRBs was 0.9 m for IB while it reduced to 0.64 m for IDB.

Table 8 Input ground motion for BM#3

Waveform ID	Earthquake Name & Station	Country	Mw	Fault Mechanism	Distance to Rupture Plane [km]	PGA [g]	PGV [m/s]
180	Imperial Valley-Array #5	U.S.A	6.53	strike slip	3.95	0.36	0.746
182	Imperial Valley-Array #7	U.S.A	6.53	strike slip	0.56	0.45	1.132
879	Landers-Lucerne	U.S.A	7.28	strike slip	2.19	0.71	0.625
1044	Northridge-Newhall	U.S.A	6.69	Reverse	5.92	0.7	1.188
1063	Northridge-Rinaldi	U.S.A	6.69	Reverse	6.5	0.87	1.745
1084	Northridge-Sylmar	U.S.A	6.69	Reverse	5.35	0.72	1.222

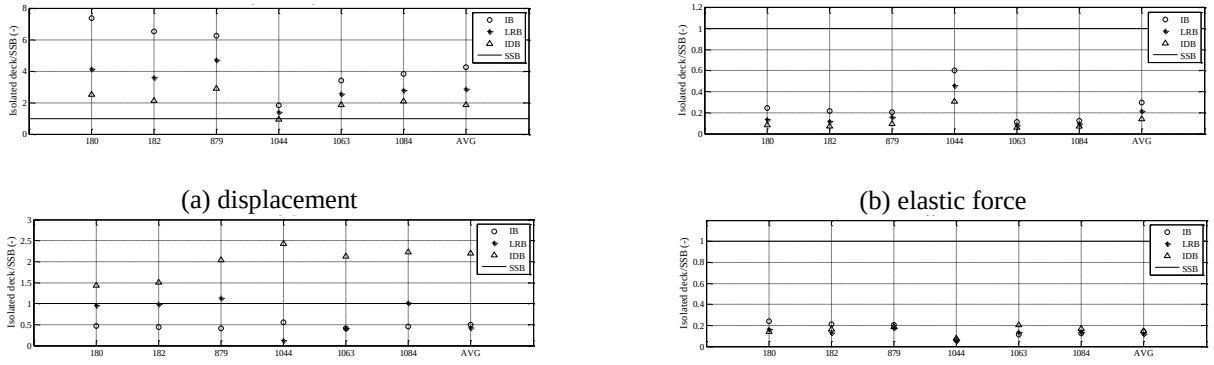

(a) displacement (b) elastic force

(d) damping force (f) base shear

Fig. 14 Normalized maximum values of BM#3 response

A set of six recorded near-fault ground motions was provided in the study of Jangid (2007) and was also used in this section for the sake of comparison (Table 8). A modified computation method was proposed by Shahi and Baker (2011) for selection of near fault ground motion in probabilistic seismic hazard analysis (PSHA).

Fig. 13 graphically shows the input motion spectra combined through square root of the sum of the squares (SRSS) approach. Sensitivity of isolated structures to near-fault ground motion can be clearly understood by comparing the spectra of Fig. 13 at flexible range period around 1 to 3 s with those given in Fig. 4(b) and Fig. 10(b).

Peak response values were obtained for SSB, IB, LRB and IDB configurations and normalized to corresponding values of SSB as depicted in Fig. 14.

Displacement response in Fig. 14(a) shows higher sensitivity of the isolated deck to near-fault motion with respect to the fixed one. Absolute displacements gave insight to this matter: under near-fault motion #180, maximum response was 0.086 m for SSB while it reached 0.64 m for IB, a very large displacement hard to be accommodated. Under the same motion, IDB displacement response was 0.21 m at peak, which suggested a steep decrease. Avarage peak displacement response is 0.11 m for SSB, 0.47 m for IB, 0.31 m for LRB and 0.2 m for IDB.

In addition to this, values of peak response displacements recorded through time-history analysis match those assumed in the preliminary design of the bearings. Similar to previous cases, pier elastic force significantly reduce for isolated mock-ups while damping force peaks at the highest value for IDB. Both acceleration response and base shear reduced of approximately 83% for isolated configurations with respect to SSB, either with or without supplemental damping system.

Even if base shear slightly increases (≈10%) considering IDB versus IB and LRB solutions, this effect is negligible in terms of global reduction with respect to fixed deck configuration.

It is worth to note that also in this case IDB demonstrated to be the most effective isolation system with significant displacement reduction with respect to both IB and LRB and negligible effect in terms of resulting base shear.

It would be also practical to compare obtained results with those of the study of Jangid (2007). In that case the same bridge under the same near-fault motions was investigated to find out the optimum value of core yield strength of LRBs, estimated in the range 15 to 20% of the weight of the structure. The equivalent period of the isolated bridge was taken in the range 2.5 to 3 s. The minimum base shear correlated to optimum value of LRB core yield strength was 2642 kN, whereas the value corresponding to IDB is 2510 kN that is 5% lower. The significant difference arises in terms of deck displacement that was 0.35 m for LRB with optimized yield strength and 0.2 m for IDB, that is almost 50% lower.

These results confirmed the effectiveness of high viscous damping in rubber isolated bridges under near fault ground motions. In addition, it must be said that hysteresis type system like LRB or FPS could be tuned for optimum

Table 9 Cost evaluation for BM#3 and comparison with IB

	Islators cost	Dampers cost	Total	Difference
IB	€124,148	€	€124,148	0%
LRB	€148,977	€	€148,977	20%
IDB	€57,259	€119,417	€176,677	42%

strength and stiffness under near fault motion. This could compromise the seismic performance under far field or even low magnitude earthquakes. Higher strength and equivalent stiffness may be required by near fault motion to reduce maximum displacement and/or maximum base shear. Therefore, the system may not experience any sliding or yielding when input properties are different from near fault, simulating a non-isolated behavior.

With respect to a complete FEM model of the bridge implemented in SAP2000, the simplified 2 DOF model overestimated displacements of 5 to 10% in all analysis cases.

As far as economical assessment is concerned, required performance on IDB would imply very large dampers, whose maximum design force makes them very expensive with respect to isolators (Table 9).

Apart from this, additional 42% and 19% overall cost of IDB control system with respect to IB and LRB, respectively, is deemed satisfactorily justified by strongly improved seismic performance.

4. Conclusions

Bridge isolation technology has been continuously growing in the last decades due to satisfactory behavior of isolated structures under real earthquakes and severe code requirements for mission critical structures.

In high seismic prone areas or near fault seismicity regions, spectral displacements at isolated periods may be hard to accommodate and this could discourage practitioners from adoption of seismic isolation technology. Supplemental damping can represent a viable solution by mitigating maximum response displacements.

In the present study, three benchmark bridges with different geometry and seismic hazard levels including near fault motion were examined. Each of them was investigated in fixed deck to pier condition (SSB), isolated by HDLRBs with 10% damping (IB), isolated by LRBs with 30% damping ratio (LRB) and isolated by HDLRBs with 70% optimal damping level (IDB).

Time history analysis were conducted in OpenSees reducing BM bridges to simplified 2 DOFs models. With respect to a complete model of the bridge, it was found that such assumption did not alter results significantly for effective isolation systems. Higher sensitivity was shown by BM#3 due to near fault seismic action.

Results of the analysis demonstrated that an isolated bridge equipped with elastomeric isolators and a total equivalent damping ratio of 70% represents a very effective design solution for both mitigation of displacement demand at the isolation level and base shear reduction in the piers. Differently from buildings where higher modes are excited by higher damping levels, for isolated decks a value of damping around 70% demonstrated not to be detrimental in terms of global response thanks to predominance of the first vibration mode.

In all cases, displacements of IDB were in the order of 30 to 40% corresponding IB displacements and 60 to 70% corresponding LRB displacements, while base shear results remained practically unchanged. This effect on base shear can be explained accounting for the phase lag between elastic and viscous components. Even if additional damping increased the damping force, at the same time it further reduced pier displacements resulting in smaller elastic component.

The proposed control system was proved capable to take advantage from both isolation and supplemental damping systems in minimizing input energy and maximizing dissipated energy at the same time, thus confirming theoretical results obtained for a regular bridge. Thanks to repeatability of effective performance under both far field and near fault ground motions, as well as for both simply supported and continuous bridges, the suggested control system demonstrates both robustness and reliability in terms of effectiveness of seismic response. Provided supplemental damping determined minimum required clearance between decks thus preventing pounding, which becomes almost decisive parameter in case of retrofit of existing bridges where the originally designed clearance is only suitable for thermal variation and could not accommodate typical isolated displacements. Advantages of IDB versus IB and LRB were explained in detail for each BM bridge.

As far as economical aspects are concerned, it was expected that using damping devices would have increased the cost of the control system. On the contrary, it was proved that the decrease in design displacements reduced isolators size and, as a result, smaller and cheaper devices were needed.

It can be finally said that the cost of the suggested isolation system with supplemental damping devices would be of the same order of magnitude of a simple isolation system. This also contributes to provide competitiveness to the suggested solution to become more common.

References

AASHTO (2010), *Guide Specifications for Seismic Isolation Design*, Third Edition, American Association State Highway and Transportation Officials, Washington DC, USA.

ANAS (2016), Prezzario ANAS 2016, http://www.stradeanas.it/content/index/arg/elenco_prezzi_2016.

Buckle, I. and Monzon, E. (2011), "Seismic isolation design examples of highway bridges", NCHRP 20-7 / Task 262(M2), University of Nevada Reno, 20-7.

Chen, W.F. and Duan, L. (2014), *Bridge Engineering Handbook*, CRC Press, New York, USA.

Chiou, B., Darragh, R., Gregor, N. and Silva, W. (2008), "NGA project strong-motion database", *Earthq. Spectra*, **24**(1), 23-44.

EC8 (2004), *Eurocode 8: Design of structures for earthquake resistance Part 1: General rules, seismic actions and rules for buildings*, CEN, European Committee for Standardization.

FIP Industriale (2016), www.fipindustriale.it, Selvazzano Dentro

(PD), Italy, http://www.fipindustriale.it/public/divisione_industriale/dispositivi_antisismici/S02%20Catalogo%20SI.pdf.
Hall, J.F., Heaton, T.H., Halling, M.W. and Wald, D.J. (1995), "Near-source ground motion and its effect on flexible buildings", *Earthq. Spectra*, **11**(4), 569-605.
Iervolino, I., Galasso, C. and Cosenza, E. (2010), "REXEL: computer aided record selection for code-based seismic structural analysis", *Bull. Earthq. Eng.*, **8**(2), 399-362.
Jangid, R.S. (2007), "Optimum lead-rubber isolation bearings for near-fault motions", *Eng. Struct.*, **29**(10), 2503-2513.
Jangid, R.S. and Kelly, J.M. (2001), "Base isolation for near-fault motions", *Earthq. Eng. Struct. D.*, **30**(5), 691-707.
Jònsson, M.H., Bessason, B. and Haflidason, E. (2010), "Earthquake response of a base-isolated bridge subjected to strong near-fault ground motion", *Soil Dyn. Earthq. Eng.*, **30**(6), 447-455.
Kelly, J.M. (1997), *Earthquake-Resistant Design with Rubber*, Springer-Verlag, London.
Kelly, J.M. (1999), "The role of damping in seismic isolation", *Earthq. Eng. Struct. D.*, **28**(1), 3-20.
Liao, W.I., Loh C.H. and Lee B.H. (2004), "Comparison of dynamic response of isolated and non-isolated continuous girder bridges subjected to near-fault ground motions", *Eng. Struct.*, **26**(14), 2173-2183.
Losanno, D., Spizzuoco, M. and Serino, G. (2014), "Optimal design of the seismic protection system for isolated bridges", *Earthq. Struct.*, **7**(6), 969-999.
Makris, N. and Chang, S.P. (2000), "Effect of viscous, viscoplastic and friction damping on the response of seismic isolated structures", *Earthq. Eng. Struct. D.*, **29**(1), 85-107.
Martelli, A. and Forni, M. (2010), "Seismic isolation and protection systems", *J. Anti-Seism. Syst. Int. Soc.*, **1**(1), 35-55.
Naeim, F. (2000), "Design of seismic isolated structures: From theory to practice", *Earthq. Spectra*, **16**(3), 709-710.
NTC (2008), *Nuove norme tecniche per le costruzioni*, DM 14 gennaio 2008, Gazzetta Ufficiale n. 29 del 4 febbraio 2008 - Supplemento Ordinario n. 30, Italy.
OpenSees (2016), opensees.berkeley.edu, University of California, Berkeley, USA.
Ozbulut, O.E. and Hurlebaus, S. (2010), "Optimal design of superelastic-friction base isolators for seismic protection of highway bridges against near-field earthquakes", *Earthq. Eng. Struct. D.*, **40**(3), 273-291.
Pantelides, C.P. and Ma, X. (1998), "Linear and nonlinear pounding of structural systems", *Comput. Struct.*, **66**(1), 79-92.
Sahasrabudhe, S.S. and Nagarajaiah, S. (2005), "Semi-active control of sliding isolated bridges using MR dampers: an experimental and numerical study", *Earthq. Eng. Struct. D.*, **34**(8), 965-983.
Shahi, S.K. and Baker, J.W. (2011), "An empirically calibrated framework for including the effects of near-fault directivity in probabilistic seismic hazard analysis", *Bull. Seismol. Soc. Am.*, **101**(2), 742-755.
Shen, J., Tsai, M.H., Chang, K.C. and Lee, G.C. (2004), "Performance of a seismically isolated bridge under near-fault earthquake ground motions", *J. Struct. Eng.*, **130**(6), 861-868.
Wang, Y.P., Chung, L.L. and Liao, W.H. (1998), "Seismic response analysis of bridges isolated with friction pendulum bearings", *Earthq. Eng. Struct. D.*, **27**(10), 1069-1093.